



NATIONAL RESEARCH CENTRE  
«**KURCHATOV INSTITUTE**»  
Institute for High Energy Physics  
of the National Research Centre  
«Kurchatov Institute»

Preprint 2018–15

S.P. Denisov, V.N. Goryachev

**Energy, radial and time distributions of the charged particles at the maximum of electromagnetic showers initiated by 5-1000 GeV electrons in Fe, W and Pb**

*Submitted to the Journal of Physics:  
Conference Series*

Protvino 2018

**Abstract**

Denisov S.P., Goryachev V.N. Energy, radial and time distributions of the charged particles at the maximum of electromagnetic showers initiated by 5-1000 GeV electrons in Fe, W and Pb: NRC «Kurchatov institute» – IHEP Preprint 2018–15. – Protvino, 2018. – p. 10, figs. 5, tables 8, refs.: 16.

The results of calculations of the charged particles energy, radial and time distributions at the maximum of electromagnetic showers initiated by electrons with energies from 5 to 1000 GeV in Fe, W and Pb are presented. It is shown that the shapes of energy distributions weekly depend on the electron energy, radial distributions for different materials become close to each other if radius is expressed in  $\text{g}/\text{cm}^2$  and the time spread of the shower particles is in the picosecond range. Analysis of the data obtained allows us to conclude that a high  $Z$  material placed in a high energy electron beam can be used as a source of short and intense bunches of ultrarelativistic positrons and electrons with subpicosecond time spread.

**Аннотация**

Денисов С.П., Горячев В.Н. Энергетические, радиальные и временные распределения заряженных частиц в максимуме электромагнитных ливней, образованных электронами с энергиями от 5 до 1000 ГэВ в Fe, W и Pb: Препринт НИЦ «Курчатовский институт» – ИФВЭ 2018-15. – Протвино, 2018. – 10 с., 5 рис., 8 табл., библиогр.: 16.

В работе представлены результаты расчётов энергетических, радиальных и временных распределений заряженных частиц в максимуме электромагнитных ливней, вызванных электронами с энергиями от 5 до 1000 ГэВ в железе, вольфраме и свинце. Показано, что форма энергетических распределений слабо зависит от энергии электрона, радиальные распределения для разных материалов становятся близкими, если радиус выражен в  $\text{г}/\text{см}^2$  и временной разброс ливневых частиц находится в пикосекундной области. Анализ полученных данных позволяет заключить, что конвертор из материала с большим  $Z$ , помещённый в пучок электронов высокой энергии, может служить источником коротких и интенсивных банчей ультрарелятивистских электронов и позитронов с субпикосекундным временным разбросом.

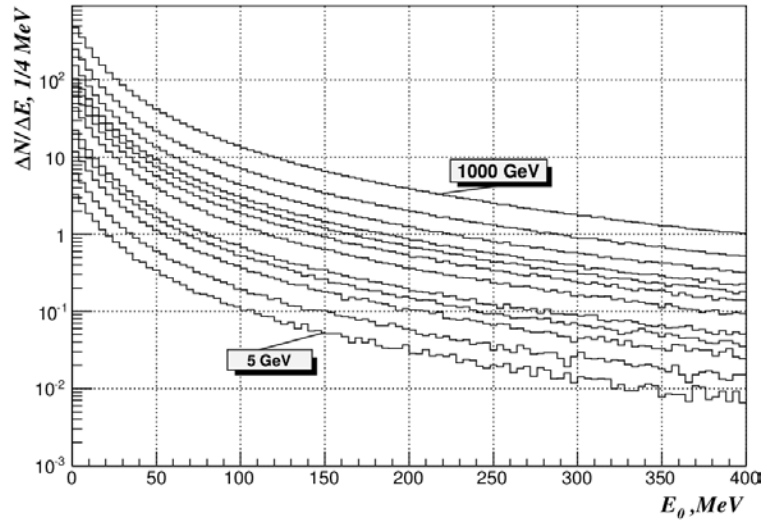
## 1. Introduction

In 1970 A.A. Tyapkin proposed to use a simple detector consisting of a lead convertor and a scintillation or Cherenkov counter behind it for  $e,\gamma$  energy measurements [1]. This idea was based on the Rossi approximation of the electromagnetic shower development [2]. As an optimal convertor thickness A.A. Tyapkin suggested to use the value  $t_{\max}$  corresponding to the maximum flux  $N_{\max}$  of the charged shower particles since  $t_{\max}$  weakly (logarithmically) depends on the energy  $E_0$  of the initial  $e,\gamma$  and  $N_{\max}$  is almost proportional to  $E_0$ . At present this type of detector is often referred to as shower maximum detector. Since 1970 a number of studies (see, for example, [3-14]) were performed to investigate shower maximum detectors characteristics like energy and space resolutions and  $e/\text{hadron}$  and  $\gamma/\pi^0$  separations which strongly depend on  $N_{\max}$  fluctuations and space and energy distributions of the charged shower particles.

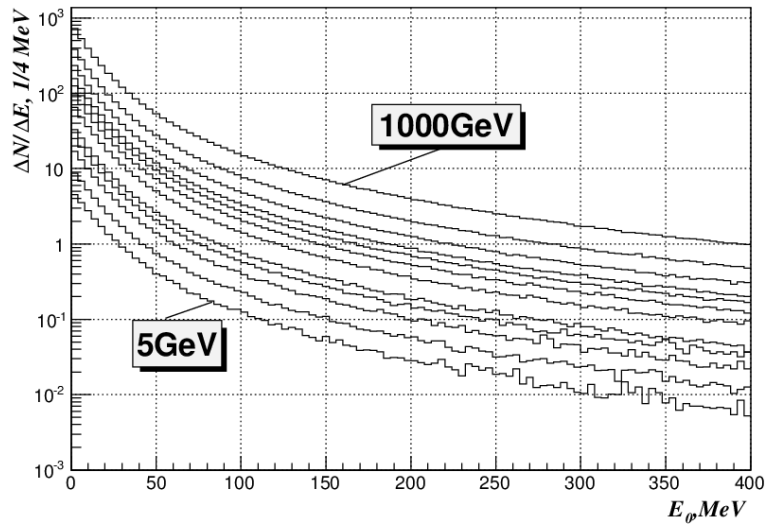
In our article [15] distributions of charge particles multiplicities at  $t_{\max}$  are considered. In this report the results of calculations of the charged particles energy, radial and time distributions in Pb, W and Fe are presented. The calculations are based on GEANT4 10.01.p02 (Physical list FTFP\_BERT) [16] with 700 micron range cut for all materials. Corresponding energy thresholds for  $e^+$  and  $e^-$  are close to 1 MeV for Pb and Fe and 1.6 MeV for W. Increase or decrease the range cut by a factor of two does not affect  $N_{\max}$  value within 0.5% statistical uncertainty [15] since the energy thresholds are much less than the average particle energy of  $\sim 50$  MeV (see below). Note that the charged particles flux at  $t_{\max}$  consists mainly of  $e^+$ ,  $e^-$ . For example, the admixture of other particles at  $E_0=200$  GeV is 0.02% only [15]. Diameter of all converters studied is 70 cm.

## 2. Energy distributions

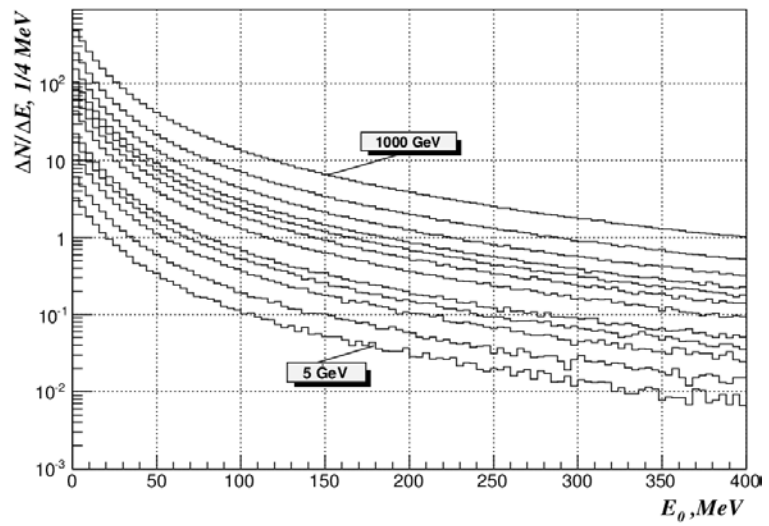
Differential energy distributions of the charged particles at  $t_{\max}$  are shown in Fig.1. Their shapes weakly depend on the electron energy  $E_0$ . The same conclusion follows from integrated distributions presented in Tables 1-3. For example, the fraction of particles with energy below 50 MeV is varied from 0.742 to 0.752 (Fe), from 0.792 to 0.806 (W) and from 0.799 to 0.810 (Pb) when  $E_0$  is changed from 5 to 1000 GeV.



**Fe**



**W**



**Pb**

Fig. 1. Energy distributions of the charge particles at  $t_{\text{max}}$ .

Table 1. Fraction of particles with kinetic energy below  $E$  at  $t_{\max}$  in Fe.

$E_0$ , GeV	$E$ , MeV									
	5	10	20	30	50	100	200	300	500	1000
5	0.199	0.341	0.519	0.624	0.742	0.864	0.938	0.964	0.984	0.996
10	0.202	0.344	0.522	0.626	0.744	0.863	0.936	0.961	0.981	0.994
20	0.206	0.350	0.525	0.629	0.745	0.863	0.934	0.960	0.980	0.993
30	0.207	0.351	0.528	0.631	0.747	0.863	0.934	0.959	0.979	0.992
40	0.207	0.352	0.529	0.632	0.746	0.863	0.933	0.958	0.978	0.992
80	0.210	0.355	0.531	0.634	0.748	0.863	0.932	0.957	0.977	0.991
120	0.211	0.356	0.532	0.634	0.748	0.862	0.932	0.957	0.977	0.991
160	0.212	0.357	0.534	0.636	0.750	0.863	0.932	0.957	0.977	0.991
200	0.213	0.359	0.535	0.638	0.751	0.864	0.932	0.957	0.977	0.991
300	0.214	0.361	0.537	0.639	0.752	0.864	0.932	0.956	0.976	0.990
500	0.215	0.362	0.539	0.640	0.752	0.864	0.932	0.956	0.976	0.990
1000	0.216	0.363	0.539	0.640	0.752	0.863	0.931	0.955	0.975	0.989

Table 2. Fraction of particles with kinetic energy below  $E$  at  $t_{\max}$  in W.

$E_0$ , GeV	$E$ , MeV									
	5	10	20	30	50	100	200	300	500	1000
5	0.210	0.364	0.561	0.673	0.792	0.901	0.959	0.978	0.991	0.998
10	0.214	0.371	0.568	0.679	0.794	0.900	0.957	0.976	0.989	0.997
20	0.222	0.381	0.577	0.688	0.801	0.903	0.958	0.976	0.988	0.996
30	0.222	0.381	0.576	0.686	0.799	0.901	0.956	0.974	0.987	0.995
40	0.224	0.384	0.580	0.689	0.801	0.902	0.956	0.974	0.987	0.995
80	0.229	0.388	0.584	0.691	0.802	0.901	0.955	0.973	0.986	0.995
120	0.230	0.390	0.586	0.694	0.804	0.902	0.955	0.972	0.986	0.994
160	0.231	0.391	0.586	0.693	0.803	0.901	0.954	0.972	0.985	0.994
200	0.231	0.391	0.586	0.693	0.803	0.901	0.954	0.972	0.985	0.994
300	0.234	0.395	0.590	0.697	0.805	0.902	0.955	0.972	0.985	0.994
500	0.236	0.397	0.592	0.698	0.806	0.902	0.954	0.972	0.985	0.994
1000	0.234	0.395	0.588	0.694	0.802	0.899	0.952	0.970	0.983	0.993

Table 3. Fraction of particles with kinetic energy below  $E$  at  $t_{\max}$  in Pb.

$E_0$ (GeV)	$E$ (MeV)									
	5	10	20	30	50	100	200	300	500	1000
5	0.217	0.373	0.570	0.682	0.799	0.905	0.961	0.978	0.991	0.998
10	0.225	0.381	0.577	0.687	0.802	0.904	0.960	0.977	0.989	0.997
20	0.229	0.385	0.580	0.690	0.802	0.904	0.958	0.976	0.988	0.996
30	0.230	0.387	0.582	0.691	0.803	0.903	0.957	0.975	0.988	0.996
40	0.233	0.390	0.585	0.693	0.803	0.903	0.957	0.974	0.987	0.996
80	0.237	0.396	0.589	0.696	0.806	0.904	0.957	0.974	0.987	0.995
120	0.238	0.396	0.590	0.696	0.805	0.903	0.956	0.973	0.986	0.995
160	0.240	0.399	0.593	0.699	0.808	0.905	0.957	0.974	0.986	0.995
200	0.240	0.400	0.592	0.699	0.807	0.904	0.956	0.973	0.986	0.995
300	0.243	0.403	0.595	0.701	0.809	0.905	0.956	0.973	0.986	0.995
500	0.244	0.404	0.597	0.702	0.810	0.905	0.956	0.973	0.986	0.994
1000	0.246	0.406	0.598	0.703	0.810	0.904	0.955	0.972	0.985	0.994

Fig. 2 demonstrates the dependencies of the average particle energy  $\langle E \rangle$  vs  $E_0$ .

They are fitted to the formula

$$\langle E \rangle = f_1 \cdot \ln E_0 + f_2, \quad (1)$$

where  $f_1$  and  $f_2$  are free parameters (see Table 4).

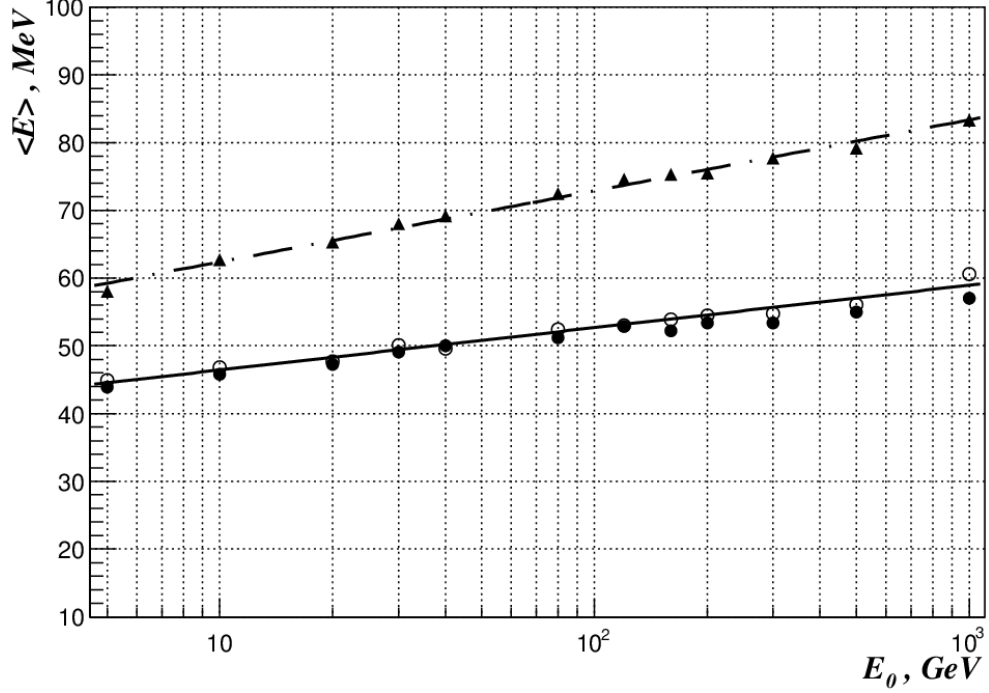


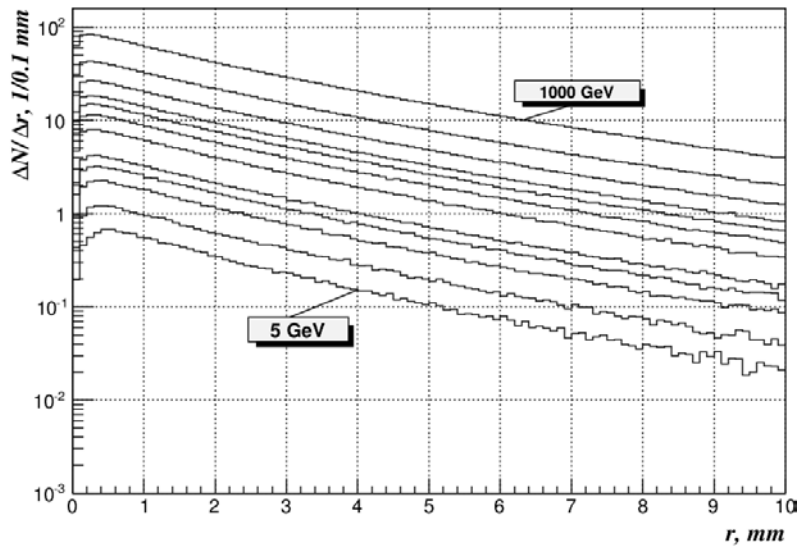
Fig. 2. Average particle energy at  $t_{\max}$  for Fe ( $\blacktriangle$ ), W ( $\circ$ ) and Pb ( $\bullet$ ). The solid and dash-dotted lines represent the fit to equation (1) for W and Fe with parameters shown in Table 4. The results for W and Pb almost coincide with each other.

Table 4. Values of  $f_1$  and  $f_2$  parameters in the formula (1),  $E_0$  is in GeV.

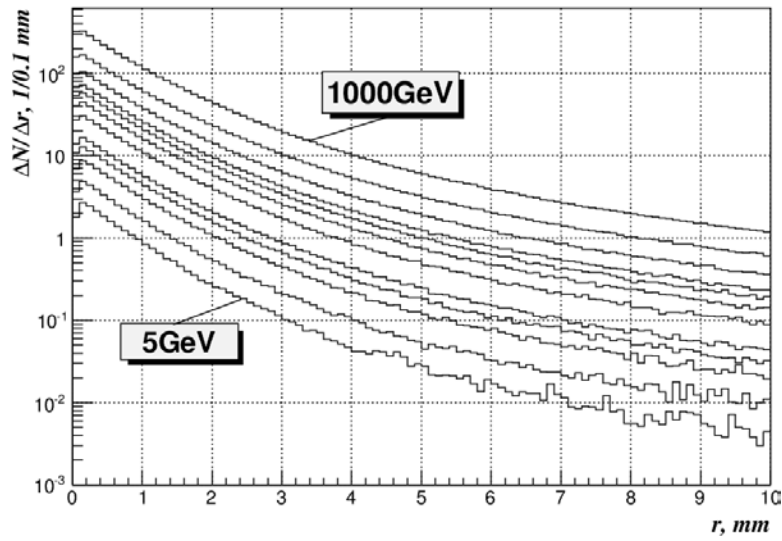
Material	Fe	W	Pb
$f_1$ , GeV	$4.55 \pm 0.13$	$2.71 \pm 0.15$	$2.39 \pm 0.10$
$f_2$ , GeV	$51.92 \pm 0.61$	$40.19 \pm 0.68$	$40.52 \pm 0.47$

### 3. Radial distributions

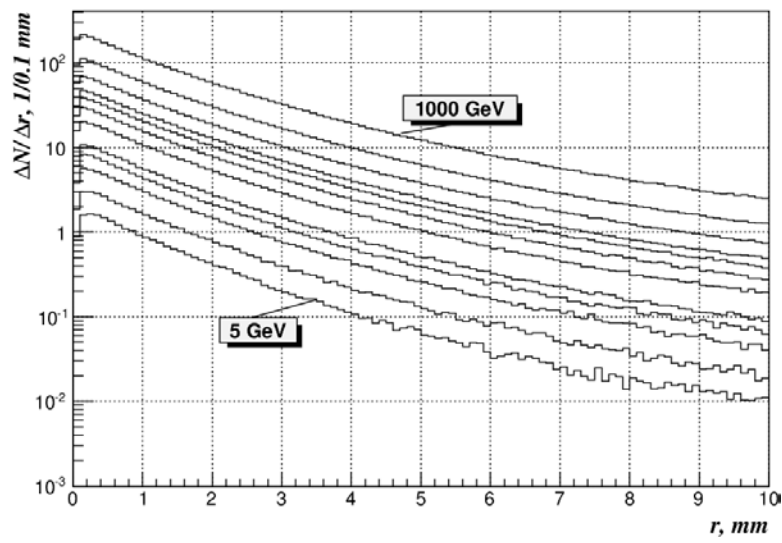
Radial distributions of the charge particles at  $t_{\max}$  are shown in Figs. 3, 4 and Tables 5-7. They are rather narrow: a circle with a radius of 1 mm contains from 66% to 59% (W) and from 48% to 44% (Pb) of particles in the 5 to 1000 GeV energy range.



**Fe**



**W**



**Pb**

Fig. 3. Radial distributions of the charge particles at  $t_{\max}$ .

Table 5. Fraction of particles inside a circle of radius  $r$  at  $t_{max}$  in Fe.

$E_0$ , GeV	$r$ , mm									
	0.5	1	2	3	5	10	20	30	50	100
5	0.127	0.284	0.511	0.652	0.812	0.940	0.980	0.988	0.993	0.997
10	0.136	0.285	0.501	0.641	0.801	0.933	0.977	0.986	0.992	0.997
20	0.139	0.283	0.494	0.631	0.789	0.926	0.976	0.986	0.992	0.997
30	0.140	0.282	0.488	0.625	0.784	0.923	0.974	0.985	0.992	0.997
40	0.142	0.281	0.485	0.621	0.780	0.920	0.973	0.985	0.992	0.997
80	0.143	0.280	0.480	0.614	0.772	0.916	0.971	0.983	0.991	0.997
120	0.144	0.280	0.479	0.612	0.770	0.913	0.970	0.983	0.991	0.997
160	0.143	0.277	0.474	0.608	0.766	0.911	0.969	0.982	0.991	0.997
200	0.143	0.276	0.472	0.605	0.763	0.909	0.968	0.982	0.991	0.997
300	0.142	0.274	0.468	0.600	0.758	0.906	0.967	0.981	0.991	0.997
500	0.143	0.274	0.466	0.597	0.755	0.903	0.966	0.981	0.990	0.997
1000	0.145	0.275	0.466	0.596	0.753	0.901	0.965	0.980	0.990	0.996

Table 6. Fraction of particles inside a circle of radius  $r$  at  $t_{max}$  in W.

$E_0$ , GeV	$r$ , mm									
	0.5	1	2	3	5	10	20	30	50	100
5	0.417	0.655	0.851	0.919	0.961	0.982	0.990	0.992	0.995	0.998
10	0.409	0.641	0.841	0.912	0.957	0.981	0.989	0.992	0.994	0.997
20	0.392	0.620	0.823	0.899	0.951	0.978	0.988	0.991	0.994	0.997
30	0.395	0.620	0.822	0.898	0.950	0.978	0.988	0.991	0.993	0.997
40	0.390	0.614	0.817	0.894	0.948	0.977	0.988	0.991	0.993	0.997
80	0.385	0.606	0.809	0.888	0.944	0.975	0.987	0.990	0.993	0.996
120	0.382	0.601	0.804	0.885	0.942	0.974	0.986	0.990	0.993	0.996
160	0.383	0.601	0.803	0.883	0.941	0.974	0.986	0.989	0.992	0.996
200	0.382	0.600	0.802	0.882	0.940	0.974	0.986	0.989	0.992	0.996
300	0.377	0.593	0.796	0.878	0.937	0.972	0.986	0.989	0.992	0.996
500	0.375	0.589	0.792	0.874	0.935	0.972	0.985	0.989	0.992	0.996
1000	0.375	0.594	0.794	0.875	0.935	0.971	0.985	0.989	0.992	0.996

Table 7. Fraction of particles inside a circle of radius  $r$  at  $t_{max}$  in Pb.

$E_e$ , GeV	$r$ , mm									
	0.5	1	2	3	5	10	20	30	50	100
5	0.270	0.481	0.718	0.830	0.920	0.969	0.985	0.989	0.993	0.997
10	0.268	0.473	0.704	0.818	0.912	0.966	0.984	0.989	0.992	0.997
20	0.264	0.463	0.691	0.805	0.903	0.962	0.982	0.988	0.992	0.997
30	0.266	0.462	0.687	0.801	0.899	0.961	0.982	0.987	0.991	0.996
40	0.264	0.458	0.683	0.797	0.897	0.959	0.981	0.987	0.992	0.996
80	0.260	0.450	0.673	0.788	0.890	0.956	0.980	0.986	0.991	0.996
120	0.260	0.449	0.670	0.785	0.888	0.955	0.979	0.986	0.991	0.996
160	0.257	0.444	0.665	0.780	0.884	0.953	0.979	0.986	0.991	0.996
200	0.257	0.444	0.664	0.780	0.884	0.953	0.979	0.986	0.991	0.996
300	0.254	0.440	0.659	0.775	0.880	0.951	0.978	0.985	0.991	0.996
500	0.254	0.437	0.655	0.771	0.877	0.949	0.977	0.985	0.990	0.996
1000	0.254	0.436	0.652	0.767	0.874	0.948	0.977	0.985	0.990	0.995



Radial distributions for different materials become close to each other if radius is expressed in  $\text{g/cm}^2$  (see Fig.4). The following formula was used to fit the integral distributions shown in Fig.4:

$$f(r) = 1 - f_0 \cdot e^{-sr} - (1 - f_0) \cdot e^{-t \cdot r}, \quad (2)$$

where  $f_0$ ,  $s$  and  $t$  are free parameters (see Table 8).

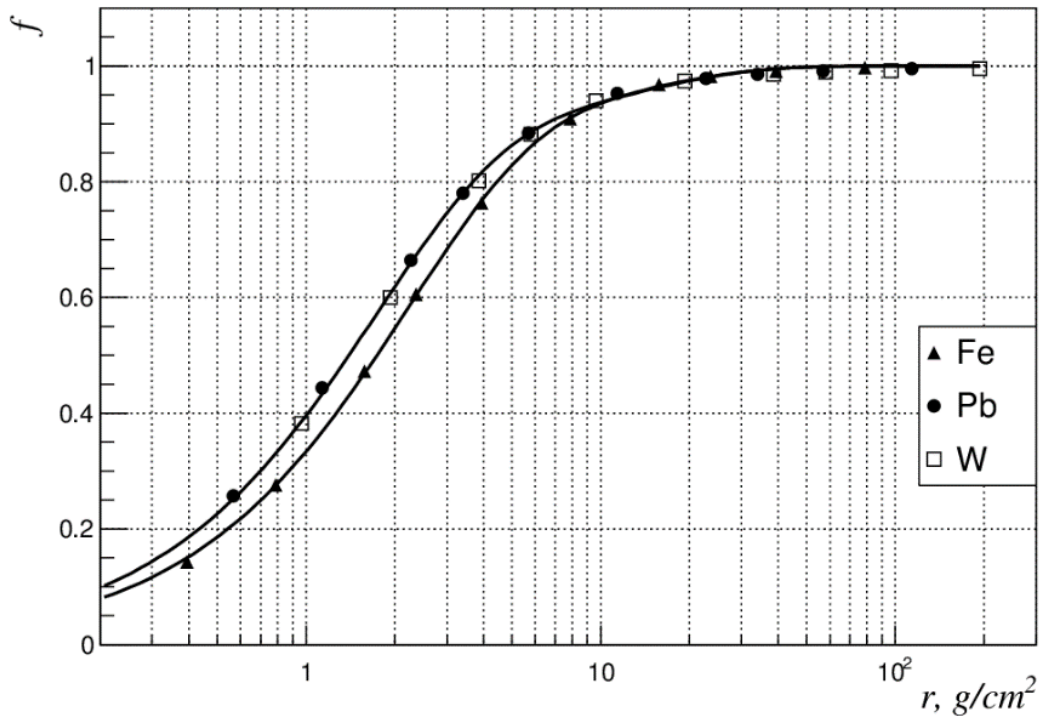


Fig. 4. Fraction of particles inside the ring of radius  $r$  for  $E_0=200$  GeV. The curves present the fit to eq. (2) for W and Pb (top) and Fe (bottom) with parameters shown in Table 8.

Table 8. Parameters values in the formula (2),  $r$  is in  $\text{g/cm}^2$ .

Material	$f_0$	$s$	$t$
Fe	0.13	0.085	0.47
Pb, W	0.14	0.086	0.59

## 4. Time distributions

Time distributions of the charged particles for 200 GeV showers in W are shown in Fig. 5. They are extremely narrow: 90% of particles are in the time window of 4 ps. For the 90% of particles inside a circle of  $r = 1\text{mm}$  the time spread is equal to 0.8 ps.

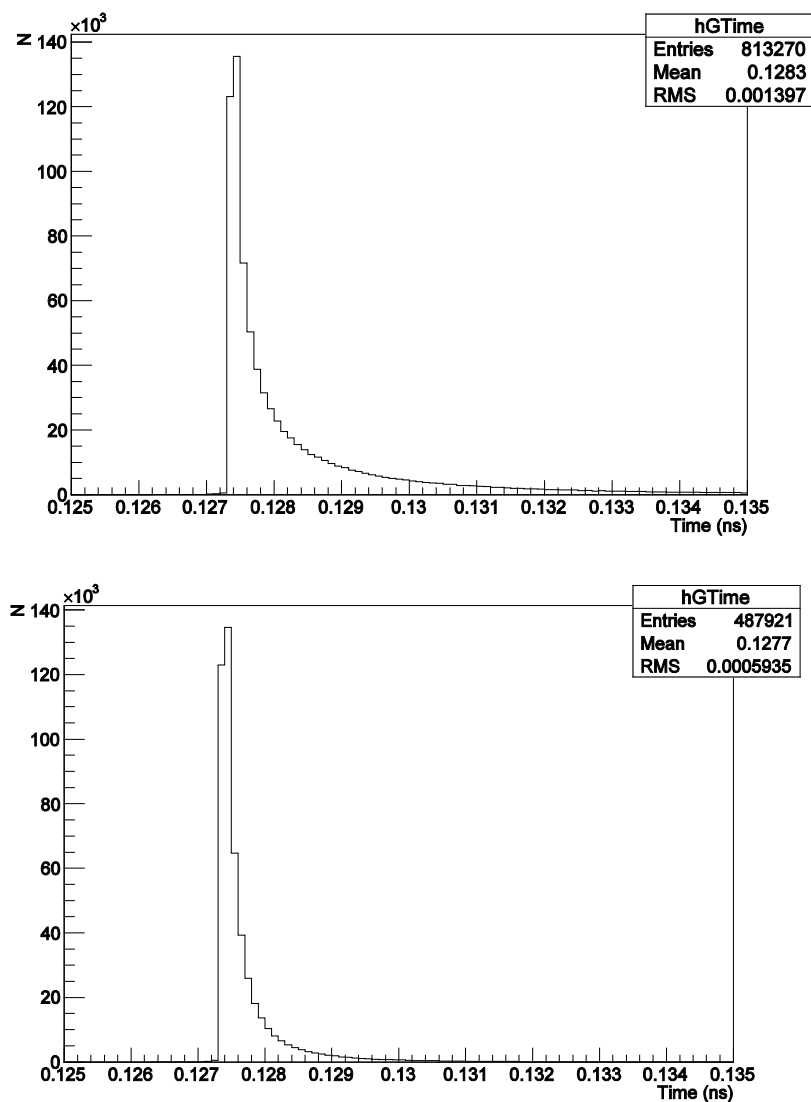


Fig. 5. Time distributions for all charged particles (top) and those inside 1 mm circle (bottom) at  $t_{\max}$  for W converter and  $E_0=200$  GeV.

## 5. Conclusions

Calculations of the energy, radial and time distributions of the charge particles at the maximum of electromagnetic showers initiated by 5 to 1000 GeV electrons in Fe, W, and Pb are performed using GEANT4. It is shown that the shapes of energy distributions and the average particle energy weakly depend on the incident particle energy and radial distributions for different materials become close to each other if radius is expressed in  $\text{g/cm}^2$ . The radial and time distributions appeared to be narrow. For example, 200 GeV incident electron produces at  $t_{\text{max}}$  in W about  $5 \cdot 10^2$  particles within the radius  $r < 1$  mm. Their time spread is 0.8 ps and average energy is 82 MeV. Thus a high  $Z$  converter with thickness of  $t_{\text{max}}$  placed in a high energy electron beam can be used as a source of short and intense bunches of ultrarelativistic positrons and electrons with subpicosecond time spread.

## Acknowledgment

We gratefully acknowledge the help of D.S. Denisov, T.Z. Gurova, A.V. Kozelov and D.A. Stoyanova in preparation of this manuscript. This work was supported in part by the Russian Foundation for Basic Research under grant № 17-02-00120.

## References

- [1] A. A. Tyapkin, NIM 85 (1970) 277-278.
- [2] B. Rossi, High energy particles (GITTL, Moscow, 1968) p. 210 (in Russian).
- [3] Ts. A. Amatuni, S. P. Denisov, R. N. Krasnokutsky et al., NIM **203** (1982) 179-182.
- [4] Ts. A. Amatuni, Yu. M. Antipov, S. P. Denisov et al., NIM **203** (1982) 183-187.
- [5] G. Apollinari, N. D. Giokaris, K. Goulianos et al., NIM A **324** (1993) 475-481
- [6] Acosta, B. Bylsma, L. S. Durkin et al., NIM A **354** (1995) 296-308.
- [7] S.J. Alvsvaag , O.A. Maeland, A. Klovning et al., NIM A **360** (1995) 219-223.
- [8] K. Byrum , J. Dawson , L. Nodulman et al., NIM A **364** (1995) 144-149.
- [9] S. A. Akimenko, V. I. Belousov, B. V. Chujko et al., NIM A **365** (1995) 92-97.
- [10] J. Grunhaus, S. Kananov, C. Milststene, NIM A **335** (1993) 129-135.
- [11] J. Grunhaus, S. Kananov, C. Milststene, NIM A **354** (1995) 368-375.
- [12] K. Kawagoe, Y. Sugimoto, A. Takeuchi et al., NIM A **487** (2002) 275–290.

- [13] S. Itoh, T. Takeshita, Y. Fujii, F. Kajino et al., NIM A **589** (2008) 370–382.
- [14] A. Ronzhin, S. Los, E. Ramberg et al., NIM A **795** (2015) 288-292.
- [15] S. P. Denisov, V. N. Goryachev, Physics of Atomic Nuclei **81**(2018) No.11, 1-6.
- [16] S. Agostinelli et al, NIM A **506** (2003) 250-303, <http://cern.ch/geant4>

*Received December 3, 2018.*

С.П. Денисов, В.Н. Горячев

Энергетические, радиальные и временные распределения заряженных частиц в максимуме электромагнитных ливней, образованных электронами с энергиями от 5 до 1000 ГэВ в Fe, W и Pb.

Препринт отпечатан с оригинала-макета, подготовленного авторами.

---

Подписано к печати 05.12.2018. Формат 60 × 84/16. Цифровая печать.  
Печ.л. 0, 85. Уч. изд.л. 1,15. Тираж 80. Заказ 16. Индекс 3649.

---

НИЦ «Курчатовский институт» – ИФВЭ  
142281, Московская область, г. Протвино, пл. Науки, 1

www.ihep.ru; библиотека <http://web.ihep.su/library/pubs/all-w.htm>

Индекс 3649

---

ПРЕПРИНТ 2018-15,  
НИЦ «Курчатовский институт – ИФВЭ», 2018

---